UNIVERSITÉ DE GENÈVE
FACULTY OF SCIENCE
Department of Astronomy

Evolution of Massive Stars with Internal Gravity Waves

Marchand Maxime, University of Geneva, 1st year Master

Under the supervision of
Moyano Facundo D., Eggenberger Patrick, University of Geneva, Stellar evolution group (GESEG)

Abstract

This report presents the work done in the context of the 1st year Master laboratories in the department of Astronomy of the University of Geneva. Numerical implementations have been added to the Geneva Stellar Evolution Code (GENEC) in order to investigate the impact of internal gravity waves (IGWs) in the chemical mixing in massive stars of 3, 7, and 20 $M_{\odot}$, as they are evolving on the main sequence.

Contents

1 Introduction

1.1 Evolution and structure of massive stars on the main sequence

In this section, we recall very briefly the different concepts to keep in mind in the context of our study. The reader that would want to read more on the theory of stellar evolution could consult the book of Kippenhahn et al. (2012) [1] for more details.

One of the most important parameter that determines the evolution of a star is its mass. Stars are usually categorised in different mass ranges that separates them according to their evolution ; intermediate mass stars ($2\ M_\odot \lesssim M \lesssim 8\ M_\odot$) are not able to burn chemical elements above carbon and oxygen, and are destined to contract into white dwarfs. On the other hand, massive stars ($M \gtrsim 8\ M_\odot$) are able to burn carbon and oxygen, and usually end their life exploding as a supernova.

When entering on the main sequence, a star roughly consists of a hydrogen burning core, and a hydrogen envelope, as illustrated in Fig. 1 on the top panel.

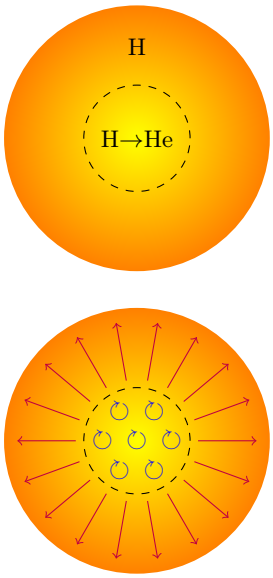

Figure 1: Structure of a massive star on the main sequence (not to scale). The top panel shows the chemical regions, that consist of a hydrogen burning core and a hydrogen envelope. The bottom panel shows the zones in the star according to the energy transport process : the circular arrows correspond to the convective core, and the straight arrows represent the radiative envelope.

At the center of the star, energy is produced through the burning of hydrogen into helium. This nuclear reaction is usually driven by the P-P chains, but when the star is massive enough, this process is made through the CNO cycle. As the energy production rate $\varepsilon_{\rm PP}$ for the P-P chain is proportional to the temperature as $\varepsilon_{\rm PP} \propto T^4$, the energy production rate for CNO cycle depends on the temperature as $\varepsilon_{\rm CNO} \propto T^{17}$. The amount of energy that is produced is so huge that radiation alone is not sufficient enough to transport all this energy. It will thus be transported by convection. The structure of a massive star is thus made of a convective core, and a radiative envelope, as illustrated in Fig. 1 on the bottom panel. Note that the structure is not the same for low mass stars, that have a radiative core, and a convective envelope, like the Sun.
It is also of importance to mention that other physical processes have a significant impact on the evolution of massive stars, such as mass-loss (which can dominate for very massive stars ($M \gtrsim 80\ M_\odot$)), and sometimes rotation ; massive stars are usually seen rotating fast.

1.2 Chemical mixing in stars & Internal Gravity Waves (IGWs)

The mixing of chemical elements in stars has a high impact on their life, both regarding their evolution and observable properties. It can transport chemical species from the outer parts of the star – like the radiative envelope – to the central regions, bringing fuel for the nuclear reactions, thus increasing the lifetime on the main sequence and the size of the burning core. It can also transport chemical elements from the core to the surface, that can modify its spectroscopic properties. One of the principal – and most understood – physical effect that can drive chemical mixing is stellar rotation [2]. For comparison, Fig. 2 presents the HR diagrams for a 20 $M_\odot$ star, at solar metallicity ($Z = 0.014$) evolving with (dashed line) and without (dotted line) rotation.

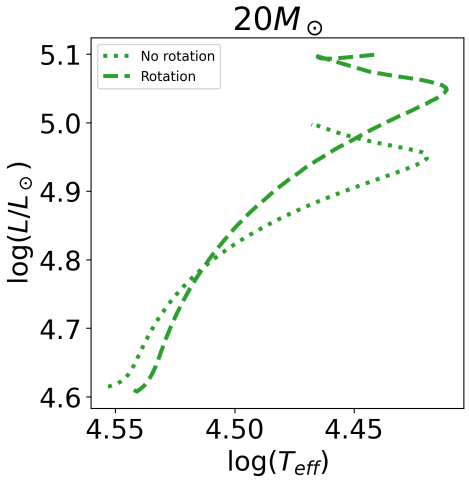

Figure 2: HR diagram for a 20 $M_\odot$ at solar metalicity ($Z = 0.014$). The dashed line is the evolution of the star with rotation, and the dotted line is the evolution without rotation.

Furthermore, there seems to be a clear relation between the projected stellar rotation speed $v \sin(i)$, and the nitrogen abundance at the surface of stars, as

shown by Fig. 3, taken from the article of Hunter et al. (2008) [3].

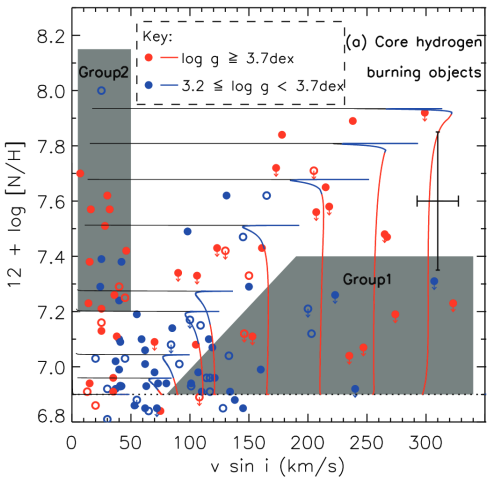

Figure 3: This figure is taken from Hunter et al. (2008) [3]. It shows the nitrogen surface enrichment $12 + \log(N/H)$ as a function of the projected stellar rotation speed $v \sin(i)$. The red dots correspond to young stars, and the blue ones are for older stars. It also presents two grey areas, the first one corresponding to older stars that have a high projected rotational velocity, but present low nitrogen enrichment (group 1), and the second one that corresponds to young stars having low projected rotation velocity, but with a high enrichment in nitrogen (group 2).

Fig. 3 presents stars that are likely to be in the main sequence of their evolution. As one can observe, a large fraction of the stars tends to follow a linear relation between their nitrogen surface abundance, and their projected rotational velocity. One can also observe two regions in this figure, one consisting of old stars (blue dots) with low nitrogen enrichment (group 1), the other one consisting of young stars (red dots) with a high nitrogen enrichment (group 2). Both of these two groups appears to behave in a different way that what is described by rotating models. This motivates the investigation of other physical processes that could drive chemical mixing, such as IGWs.

1.3 Convective overshooting

The overshooting from the convective core is a physical process that is taken into consideration for the simulations in order to compensate the lack of accuracy in the modelisation of chemical mixing and convection. The boundary of the convective core is usually described by the Schwarzschild criterion, which describes the dynamical stability of a fluid element that is adiabatically displaced. The criteria of stability is defined as $\nabla_{\rm rad} < \nabla_{\rm ad}$, with $\nabla_{\rm rad}$ and $\nabla_{\rm ad}$ the radiative and adiabatic gradients. If this condition is true, then there will be no convection.[1] Physically, the Schwarzschild criterion gives the point where the acceleration of a fluid element vanishes. But it does not indicate anything regarding the velocity, meaning that the cell could be able to travel further than this limit thanks to its inertia. This effect can be implemented in the simulations by enlarging the region where the chemical elements are totally mixed, or by using a decaying diffusion coefficient from the convective boundary, which is usually called *exponential overshooting*.
The effects of convective overshooting can be quantified by the coefficient $\alpha_{\rm ov}$, which is given by :

$$\alpha_{\rm ov} = \frac{d_{\rm over}}{H_P} \tag{1}$$

Where $d_{\rm over}$ is the distance over which overshooting occurs, and H_P is the pressure scale height. $\alpha_{\rm ov}$ thus describes by how much pressure scale height the convective core is enlarged. In order to see the effects of convective overshooting on the evolution of a star, Fig. 4 presents the evolutionary tracks for 3, 7, and 20 $M_\odot$ stars on the main sequence, and compares the evolution for different values of the convective overshooting coefficient $\alpha_{\rm ov}$. The solid lines present the evolutionary track without convective overshooting ($\alpha_{\rm ov} = 0.0$), and the dashed lines are the evolution simulated with a convective overshooting coefficient of $\alpha_{\rm ov} = 0.1$.

1.4 Internal Gravity Waves

Mixing of chemical elements in stellar interiors can occur by different physical processes. For example convection in the cores of massive stars can mix chemical elements efficiently. However, in massive stars convection only occurs in the core of the star where hydrogen burning takes place. In regions where convection cannot develop, other physical processes could contribute to the transport of chemical elements. For example rotation, convective overshooting, semiconvection, among others (e.g. Salaris & Cassisi (2017) [4]). Moreover, the interaction between convection and stable radiative regions can induce chemical mixing. Convective motions can induce perturbations in the stable radiative interior which can generate waves where the restoring force is gravity. These perturbations lead to the internal gravity waves (IGW) in stellar interiors. These waves can transport energy and chemical elements in stellar interiors, especially in massive stars where the convective cores are larger (e.g. Rogers & McElwaine (2017) [5], Varghese et al. (2023) [6]).

[1] In regions where the chemical composition is not homogeneous, one makes use of the Ledoux criteria, which is given by $\nabla_{\rm rad} < \nabla_{\rm ad} + \frac{\varphi}{\delta} \nabla_\mu$. The Schwarzschild criteria is thus a particular case of the Ledoux criterion, used in regions where $\nabla_\mu = 0$.

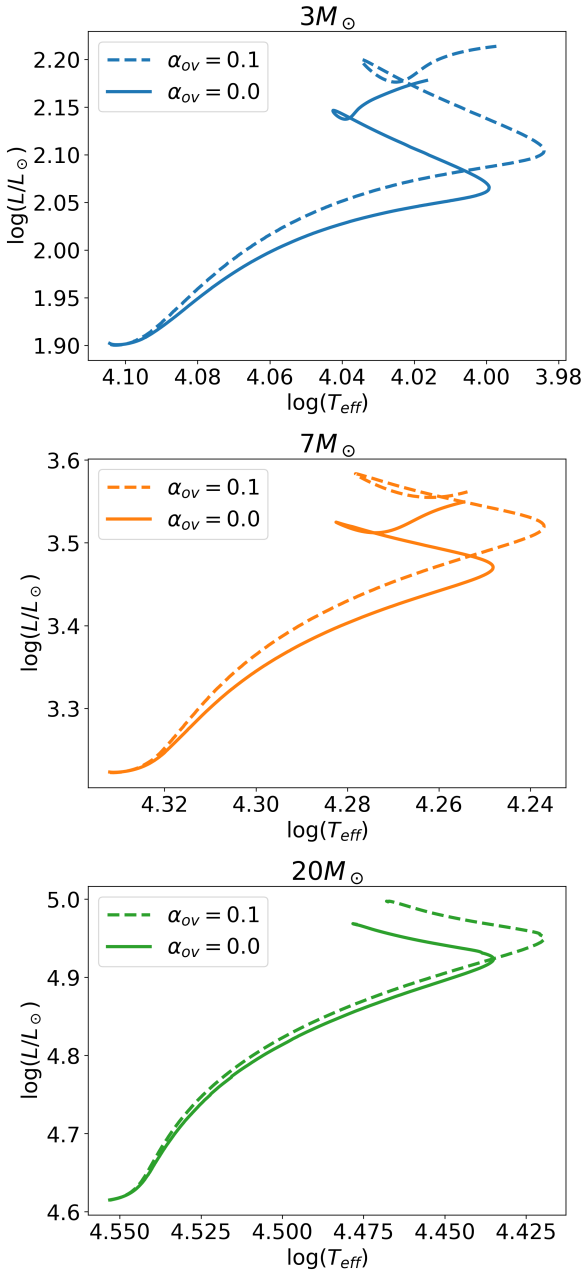

Figure 4: HR diagrams for 3, 7 and 20 $M_\odot$ stars. The simulations does not go further than the end of the main sequence. Solid lines are simulations made with a convective overshooting coefficient of $\alpha_{ov} = 0.0$ (no overshooting). The dashed lines are for stars with $\alpha_{ov} = 0.1$

Moreover, it was shown that the chemical mixing induced by IGW can be included in stellar evolution codes as a diffusive process, such as turbulent processes like convection (Varghese et al. (2023) [6]). Thanks to these properties, the effects of chemical mixing by IGW can be explored through the evolution of stars and evaluate their impact and the compatibility with previously established chemical-mixing processes, such as rotation (e.g. Maeder & Meynet (2000) [2]).

2 Method

In this section, we present which tools and methods we used in order to simulate the effects of IGWs in the evolution of stars.

Background

In this project, we have made use of the results from the article of Varghese et al. (2023) [6]. They studied the chemical mixing through IGWs by running 2D hydrodynamical simulations in stellar models of 3, 7, and 20 $M_\odot$ that were generated by MESA [7]. They have made use of tracer particles, that allowed them to study in detail the chemical mixing in the stars, and were able to generate diffusion profiles as a function of the radius for the three stellar masses, at different epochs on the main sequence.

Numerical simulations & chemical mixing

In this project, we have made use of the Geneva Stellar Evolution Code (GENEC) [8] to run our simulations. Given an initial state, GENEC simulates the evolution of stars at different time steps by solving the four equations of stellar structure (Eqs. (2), (3), (4), (5)), that are given by[2] [1] :

$$\frac{\partial r}{\partial m} = \frac{1}{4\pi r^2 \rho} \tag{2}$$

$$\frac{\partial P}{\partial m} = -\frac{Gm}{4\pi r^4} \tag{3}$$

$$\frac{\partial l}{\partial m} = \varepsilon_n - \varepsilon_\nu - c_P \frac{\partial T}{\partial t} + \frac{\delta}{\rho}\frac{\partial P}{\partial t} \tag{4}$$

$$\frac{\partial T}{\partial m} = -\frac{GM}{4\pi r^4 P}\nabla \tag{5}$$

Where L is the luminosity, P the pressure, T the temperature, r and m are the radial- and mass-coordinates. It also solves the equation of chemical mixing for each chemical specie X_i, which is given by [9] :

$$\rho \frac{dX_i}{dt} = \frac{1}{r^2}\frac{\partial}{\partial r}\left(\rho r^2 D \frac{\partial X_i}{\partial r}\right) + \left(\frac{dX_i}{dt}\right)_{\text{nucl}} \tag{6}$$

Where r and ρ are the radius and the density, and D is the total diffusion coefficient that takes into consideration the chemical mixing in the vertical direction, such as the shear instabilities and convection. See [8] and [9] for more details. We implemented a subroutine in

[2]Note that these equations above are valid for non rotating stars, and have to be slightly modified in order to take rotation into consideration. GENEC has been developed in order to be able to compute rotating stellar models. The exact equations that are solved can be found in [8].

the code that computes the diffusion profile $D_{\rm igw}$ due to IGWs, as prescribed in the article of Varghese et al. (2023) [6], and added it to the total diffusion profile D.

Diffusion profiles

The diffusion profiles for IGWs were taken from the results of Varghese et al. (2023) [6], and can be approximated with the following formula :

$$D_{\rm igw} = A \cdot \nu^2_{\rm wave}(\omega, l, r) \tag{7}$$

In which A is a constant that has the units of seconds, ω, l and r are respectively the frequency of the waves, the angular degree and the radial coordinate, and $\nu_{\rm wave}(\omega, l, r)$ corresponds to :

$$\begin{aligned} \nu_{\rm wave}(\omega, l, r) \quad = \quad & \nu_0(\omega, l, r) \cdot \left(\frac{\rho}{\rho_0}\right)^{-\frac{1}{2}} \cdot \\ & \cdot \left(\frac{r}{r_0}\right)^{-1} \left(\frac{N^2 - \omega^2}{N_0^2 - \omega^2}\right)^{-\frac{1}{4}} e^{-\tau/2} \end{aligned} \tag{8}$$

Where $\nu_0(\omega, l, r)$ is the initial wave amplitude, ρ, r, ω and N are respectively the density, radius, frequency and Brunt-Väisälä frequency. ρ_0, r_0, and N_0 corresponds to the physical quantities, defined from the point where the waves are excited. In this work, we defined them as the values at the boundary of the convective core.

3 Results & Discussion

In this section, we present the results that we obtained from the simulations with GENEC. Before making any modifications in the code, we have made two simulations for each of the three stellar masses, by modifying the convective overshooting coefficient $\alpha_{\rm ov} = 0.0$ and $\alpha_{\rm ov} = 0.1$. We did this in order to see if the mixing by IGWs could mimic an increasing overshooting strength with mass (see for instance paper from Martinet et al. (2021) [10]). These results were already presented in section 1.3.

3.1 Constant diffusion coefficient

As a first step for this project, we studied the impact of adding a diffusion coefficient $D_{\rm igw}$ that is constant with respect to the radius. Fig. 5 presents the three evolutionary tracks for the three stellar masses, and compares the evolution of the stars with (solid lines) and without (dotted lines) the constant diffusion coefficient $D_{\rm igw}$.

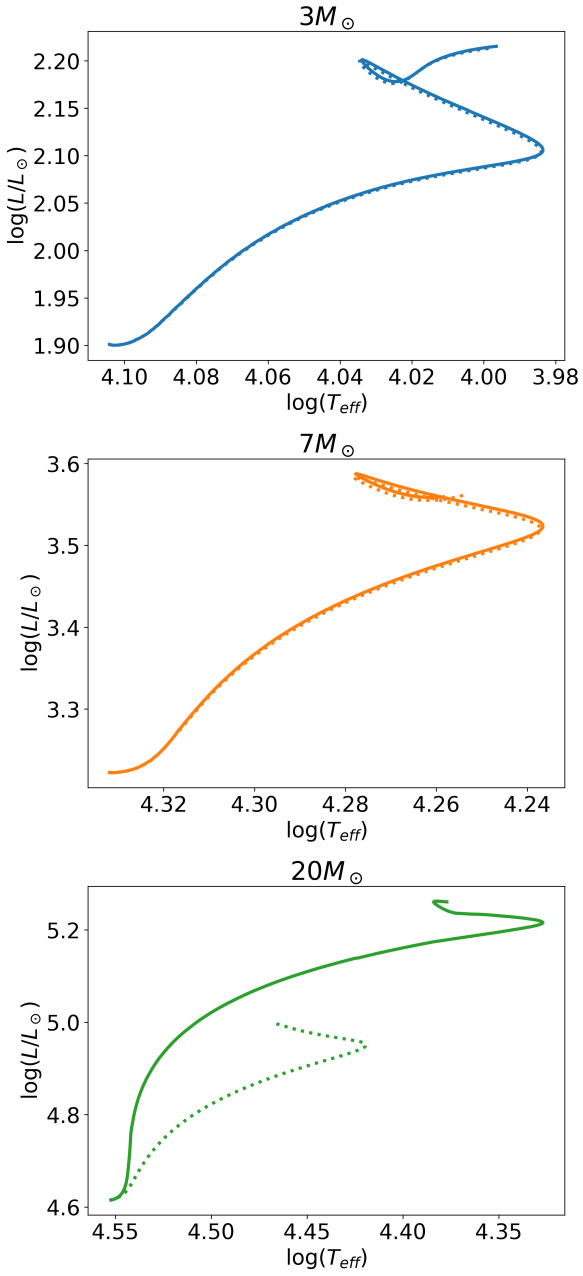

Figure 5: HR diagrams for 3, 7 and 20 $M_{\odot}$. The dotted line represents the evolutionary track from GENEC before that any modifications were made in the code (no IGWs). The solid lines are showing the evolution with a constant diffusion coefficient $D_{\rm igw}$ with the values given in Table 1.

The values were chosen according to the results presented in the article of Varghese et al. (2023) [6]. We decided to choose lower boundaries, that are presented in Table 1 :

M $[M_\odot]$	$D_{\rm igw}$ $[\rm cm^2 s^{-1}]$
3.0	$1.0 \cdot 10^1$
7.0	$1.0 \cdot 10^3$
20.0	$1.0 \cdot 10^7$

Table 1: Values chosen for the constant diffusion coefficient, according to the article of Varghese et al. (2023) [6].

On Fig. 5, one clearly sees that adding a constant diffusion coefficient in Eq. 6 does not seem to affect the 3 and 7 $M_\odot$ stars significantly. On the other hand, the effects on the 20 $M_\odot$ star are striking. One first effect is that the star evolves quasi vertically at the very beginning of the main sequence. The star is brighter, and reaches lower temperatures towards the end of the MS. It also tends to increase the lifetime on the main sequence. These effects on the HR diagrams are due to the strong mixing induced by the high diffusion coefficient employed. This can transport hydrogen to the convective core, making it larger and thus increasing the lifetime on the main sequence, and can also bring Helium to the surface, that can increase the luminosity of the star, because helium has a lower opacity than hydrogen (especially for stars with temperatures below 30000 K, where helium is not ionised).
As the effects are not easily visible for 3 and 7 $M_\odot$ stars, we will only concentrate on the effects for the 20 $M_\odot$ star in the following sections.

3.2 Diffusion profile prescribed by Varghese et al.

We now present simulations made with a diffusion profile as prescribed in the article from Varghese et al. (2023) [6]. Table 2 presents the values chosen for the initial wave amplitude $\nu_0(\omega, l, r)$, that correspond to the values of the constant diffusion coefficients presented in Table 1, and the chosen values for the frequency ω, as defined in Eqs. (7) and (8).

M $[M_\odot]$	ν_0 $[\rm cm^2\ s^{-1}]$	ω $[\mu\rm Hz]$
3.0	$1.0 \cdot 10^1$	9.0
7.0	$1.0 \cdot 10^3$	5.0
20.0	$1.0 \cdot 10^7$	4.0

Table 2: Values chosen for $\nu_0(\omega, l, r)$ and ω, from the article of Varghese et al. (2023) [6].

The values for the frequency ω were chosen according to the article of Varghese et al. (2023) [6], in order to fit well the approximation formulas given by Eqs. (7) and (8) with their simulations. Fig. 6 presents the diffusion profile as a function of the stellar radius, at the ZAMS. The light green area corresponds to the convective zone. In this convective region, chemical mixing is so efficient that it is considered to happen quasi instantaneously, and is thus not treated in Eq. (6).

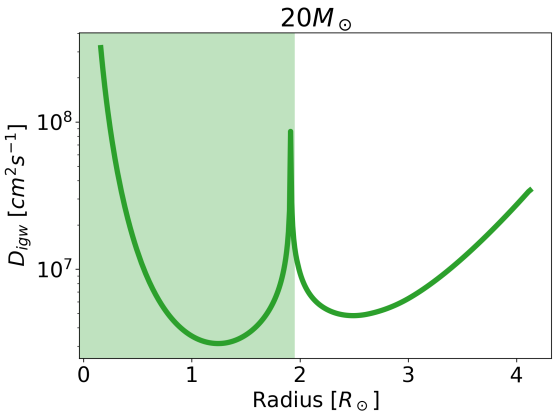

Figure 6: Diffusion profile $D_{\rm igw}$ as a function of the stellar radius for the 20 $M_\odot$ star, following the prescriptions from Varghese et al. (2023) [6]. The light green area represents the convective region in the star. In this region, the mixing is considered to be so efficient that it is treated as quasi instantaneous, meaning that it is not treated by Eq. (6).

Fig. 7 presents the HR diagrams for the 20 $M_\odot$ star (solid line). As a comparison, the figure also presents the evolutionary tracks made with GENEC before that any modifications in the code were made (dotted line), and with the constant diffusion coefficient (dashed line).

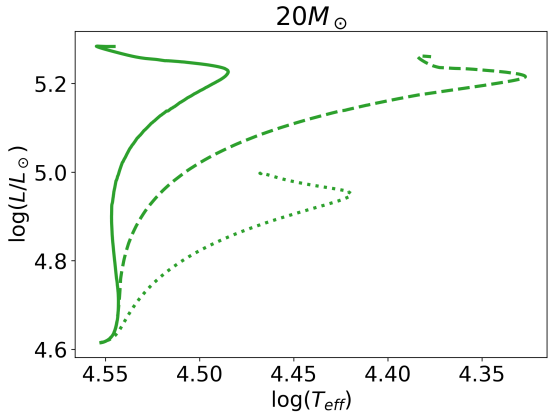

Figure 7: HR diagrams for 20 $M_\odot$ star with diffusion profiles as prescribed by Varghese et al. (solid line). For comparison, the plot also shows the simulation that was run before that any modification were made in the code (dotted line), and the simulation with a constant diffusion profile (dashed line).

One can see in Fig. 7 that the inclusion of the diffusion profile $D_{\rm igw}$ that is radius-dependant tends to increase the effect discussed in the previous section. However the evolutionary track does not reach temperatures as low as for the inclusion of the constant diffusion profile. These effects can be explained by studying the profiles of the different chemical species, and the enrichment of the chemical elements at the surface of the star, as it will be discussed in the following sections.

3.3 Chemical profiles

Fig. 8 presents the hydrogen (top panel) and Helium (bottom panel) abundances, as a function of the normalised mass. The different line styles correspond to different epochs on the main sequence ; solid line is at the ZAMS, dashed line corresponds to a central hydrogen abundance of 70%, dotted line is for 35%, and dot-dashed line is for 10%, of the total mass of the star. The green curves are from the simulation with the diffusion coefficient as prescribed in the article of Varghese et al. (2023) [6], and the orange ones are for the simulations with GENEC before that any modifications were made (no IGWs).
As one can observe, the inclusion of chemical mixing through IGWs has a clear effect on the chemical profiles. One observes much less hydrogen in the radiative envelope. One also remarks that there is a much higher abundance of helium, that can be easily seen with the lines corresponding to the middle of the main sequence.

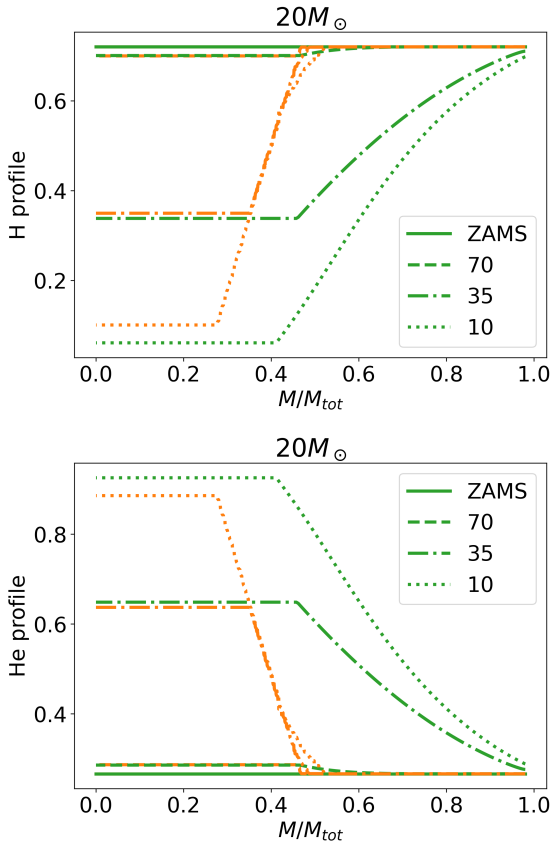

Figure 8: On the top : H abundance as a function of the normalised mass at four different epochs on the main sequence. These epochs were chosen according to the values of the central hydrogen abundance : ZAMS (solid), 70% (dashed), 35% (dash-dotted) and 10% (dotted) of the total mass of the star. The bottom panel presents the same graph, for the Helium profile.

3.4 Surface enrichment of helium and nitrogen

Fig. 9 presents the surface abundance of helium, as a function of the central hydrogen abundance (solid line). For comparison, the graph also presents the simulation with GENEC before that any modification were made in the code, meaning no IGWs (dotted line) and the simulation with the inclusion of the constant diffusion profile with the values shown in Table 1 (dashed line). As one can observe, the abundance is effectively increasing, meaning that it is transported towards the surface of the star. This confirms the conclusion that the much higher effective temperatures seen are related to the strong presence of helium at the surface of the star.

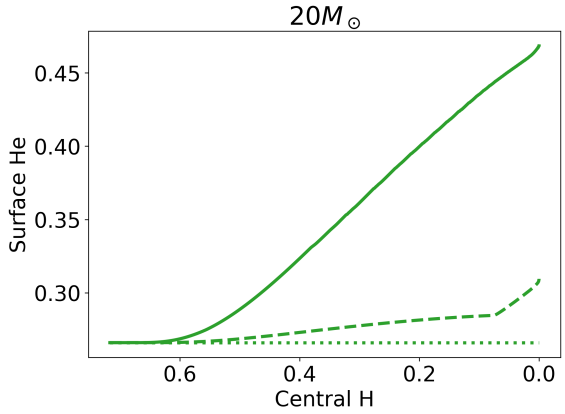

Figure 9: Evolution of the He surface abundance (in mass fraction), as a function of central H abundance. Dotted line presents the simulation made before adding any modifications to the code, dashed line is the simulation made with the implementation of the constant diffusion coefficient (c.f. Table 1) and solid line is the simulation taking into consideration the diffusion coefficient that is radius dependent, as prescribed in the article of Varghese et al. (2023) [6].

One observes that the surface abundances do not seem to match between Fig. 8 and 9. I would not be able to explain this phenomena.

Fig, 10 presents the change in nitrogen surface abundance normalised to its value at the main sequence, in log difference : $\Delta \log(N/H)$. This quantity is plotted as a function of the central hydrogen abundance (solid line). For comparison, the graph also shows the simulation without the inclusion of IGWs (dotted line), and with the inclusion of the constant diffusion coefficient (dashed line). One clearly sees that it increases during the evolution of the star, which is one more time a sign that chemical elements are transported in the star. Indeed, nitrogen is a result of the CNO cycle occuring at the center of the star. However, the value of the enrichment at the middle of the main sequence ($\sim$0.8) is much higher than what is presented in the article from Ekström et al (2012), where they find a

value of ∼0.3.

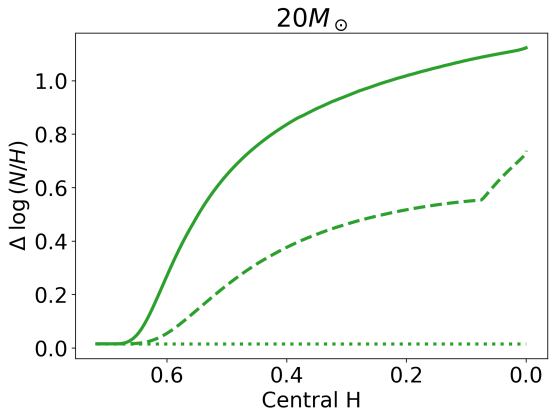

Figure 10: Change in ^{14}N surface abundance with respect to its value at the main sequence, in log difference (solid line). For comparison, the graph also shows the simulation without the inclusion of IGWs (dotted line), and the simulation with the inclusion of the constant diffusion coefficient (dashed line).

3.5 Mass fraction of the convective core

Fig. 11 presents the mass fraction of the convective core, as a function of the age (solid line). The dotted line corresponds to the simulations before that any modification was made in GENEC (no inclusion of IGWs), and the dashed line comes from the simulation with the inclusion of the constant diffusion coefficient, presented in Table 1.

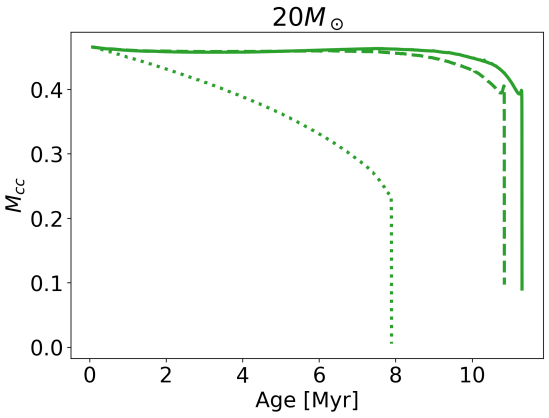

Figure 11: Evolution of the mass fraction of the convective core M_{cc}, as a function of the age (solid line). For comparison, the dotted line presents the simulation made before adding any modifications to the code (no inclusion of IGWs), and the dashed line presents the simulation with the inclusion of the constant diffusion coefficient, whose value is indicated in Table 1.

One clearly sees that the mass fraction of the convective core increases when adding the effect of IGWs in the simulations, and that it tends to live longer. This is an expected outcome, as we discussed in the previous sections that processes that conduct to chemical mixing could bring fuel in the burning part of the stars, thus increasing the size of the convective core and increase its lifetime.

4 Conclusion

In this work, we have investigated the evolution of stars when adding the effects of chemical mixing through IGWs in massive stars. For this purpose, we have made use of GENEC, in which we implemented a subroutine that computed the diffusion profiles $D_{\rm igw}$, as prescribed in the article from Varghese et al. (2023) [6].
Even if this implementation did not seem to influence the evolution for the intermediate-mass stars (3 and 7 $M_\odot$), we have found different effects of IGWs on the properties of the massive star (20 $M_\odot$). The lifetime on the main sequence appears to be longer on the HR diagram. We have found that the abundance of hydrogen is lower in the radiative envelope, as the abundance of helium is higher in the middle of the main sequence. We also found that the mass fraction of the convective core increased towards the end of the main sequence, and lived longer. Finally, we also found an enrichment in nitrogen that is much higher than what is presented in the paper from Ekström et al. (2012) [9].

References

[1] Rudolf Kippenhahn, Alfred Weigert, and Achim Weiss. *Stellar Structure and Evolution*. Astronomy and Astrophysics Library. Springer Berlin Heidelberg, Berlin, Heidelberg, 2012.

[2] Andre Maeder and Georges Meynet. The evolution of rotating stars. *Annual Review of Astronomy and Astrophysics*, 38(1):143–190, September 2000. arXiv:astro-ph/0004204.

[3] I. Hunter, I. Brott, D. J. Lennon, N. Langer, P. L. Dufton, C. Trundle, S. J. Smartt, A. de Koter, C. J. Evans, and R. S. I. Ryans. The VLT FLAMES Survey of Massive Stars: Rotation and Nitrogen Enrichment as the Key to Understanding Massive Star Evolution. *The Astrophysical Journal*, 676(1):L29–L32, March 2008.

[4] Maurizio Salaris and Santi Cassisi. Chemical element transport in stellar evolution models. *Royal Society Open Science*, 4(8):170192, August 2017.

[5] T. M. Rogers and J. N. McElwaine. On the Chemical Mixing Induced by Internal Gravity Waves. *The Astrophysical Journal*, 848(1):L1, October 2017.

[6] A. Varghese, R. P. Ratnasingam, R. Vanon, P. V. F. Edelmann, and T. M. Rogers. Chemical Mixing Induced by Internal Gravity Waves in Intermediate-mass Stars. *The Astrophysical Journal*, 942(1):53, January 2023.

[7] Bill Paxton, Lars Bildsten, Aaron Dotter, Falk Herwig, Pierre Lesaffre, and Frank Timmes. MODULES FOR EXPERIMENTS IN STELLAR ASTROPHYSICS (MESA). *The Astrophysical Journal Supplement Series*, 192(1):3, January 2011.

[8] P. Eggenberger, G. Meynet, A. Maeder, R. Hirschi, C. Charbonnel, S. Talon, and S. Ekström. The Geneva stellar evolution code. *Astrophysics and Space Science*, 316(1-4):43–54, August 2008.

[9] S. Ekström, C. Georgy, P. Eggenberger, G. Meynet, N. Mowlavi, A. Wyttenbach, A. Granada, T. Decressin, R. Hirschi, U. Frischknecht, C. Charbonnel, and A. Maeder. Grids of stellar models with rotation: I. Models from 0.8 to 120 $M_{\odot}$ at solar metallicity ($Z = 0.014$)$*$. *Astronomy & Astrophysics*, 537:A146, January 2012.

[10] S. Martinet, G. Meynet, S. Ekström, S. Simón-Díaz, G. Holgado, N. Castro, C. Georgy, P. Eggenberger, G. Buldgen, S. Salmon, R. Hirschi, J. Groh, E. Farrell, and L. Murphy. Convective core sizes in rotating massive stars: I. Constraints from solar metallicity OB field stars. *Astronomy & Astrophysics*, 648:A126, April 2021.

Figures without any indication regarding the source were self made.